Performance Study of EDM Process Parameters Using TiC/ZrSiO$_4$ Particulate-Reinforced Copper Composite Electrode

Duraisivam Saminatharaja[1,*] – Suresh Periyakgounder[2] – Mahalingam Selvaraj[3] – Jamuna Elangandhi[1]

[1]The Kavery Engineering College, Department of Mechanical Engineering, India
[2]Sona College of Technology (Autonomous), Department of Mechatronics Engineering, India
[3]Sona College of Technology (Autonomous), Department of Mechanical Engineering, India

Electrical discharge machines (EDM) are widely employed in machining components containing complex profiles of hard-to-cut and machining materials. However, the fabrication-of-tool time for the EDM process is excessively high in the traditional machining method, which significantly affects the machining rate. Therefore, in this paper, a powder metallurgy (PM) technique is employed to fabricate the tool electrode using copper (Cu), titanium carbide (TiC), and zirconium silicate (ZrSiO$_4$) for different combinations. An L18 orthogonal array (OA) is planned using the following input parameters: three types of tools (Cu, Cu$_{90}$, Cu$_{80}$), peak current (PC) [A], pulse on time (PT) [μs], and gap voltage (GV) [V]. The performance of EDM is evaluated through the material removal rate (MRR), tool wear rate (TWR), and surface roughness (SR). The process parameters are optimized using two different techniques: the technique for order of preference by similarity to the ideal solution (TOPSIS) and grey relational analysis (GRA). TOPSIS and GRA optimization techniques produce the same optimal parametric solution for less TWR, SR, and higher MRR with the combination of the Cu$_{90}$ tool, E8 APC, 15 μs pulse PT, and 75 V GV. Based on the ANOVA table of TOPSIS, pulse on time plays a major role, contributing 46.8 % of the machining performance; peak current shows the most significant contribution of 39.3 % of the machining performance using GRA values. Furthermore, the scanning electron microscope (SEM) image analyses are carried out on the machined workpiece surface to understand the effect of tools on machining quality.
Keywords: powder metallurgy, composite tool, copper, electrical discharge machine, technique for order of preference by similarity to ideal solution, grey relational analysis

Highlights
- *EDM process parameters (Gap voltage, current, pulse on time) were optimized through the L18 orthogonal experimental design method, GRA method, and the TOPSIS method considering responses, such as MRR, TWR, and SR.*
- *Based on the experiment, MRR and TWR were increased by increasing the reinforcement percentage of composite electrodes.*
- *It was revealed that the MRR value of the Cu$_{90}$ tool electrode was 0.0319 g/min, which is 1.9 times higher than the other tool electrode.*
- *Pulse on time and peak current have major contribution values (46.8 % and 39.3 %) from the ANOVA table of TOPSIS and GRA.*

0 INTRODUCTION

EDM is a widely accepted and promising process used in non-traditional machining processes. Due to its unique nature of machining characteristics, the usage of EDM has been increasing enormously in manufacturing sectors, including forging, automobile, aviation, and the biomedical and medical industries. Moreover, an excellent surface finish and precision can be made by means of EDM, in cases in which the conventional machining method fails. The stainless steel (SS) SS304 has been employed in various manufacturing sectors due to its high toughness, wear resistance, and corrosion resistance. In the EDM process, apart from electrical parameters, other parameters, such as tool modification, dielectric medium changes, tool rotational assistances and tool vibration, play vital roles in improving machining performances. Therefore, various research attempts were undertaken in the previous decade by researchers. In line with that, Sivakumar et al. [1] investigated

the EDM process parameters for oil-hardening, non-deforming tool steel (OHNS) using copper and titanium die boride composite electrodes. They developed the electrode using a powder metallurgy process and optimized the process through response surface methodology. Chakmakchi et al. [2] used a titanium alloy (Ti) as an electrode for machining the cobalt-chromium (Co-Cr) alloy and Ti6Al7Nb through the EDM process. The EDM process parameters were analysed using the evaluations of morphological and electrochemical changes in the workpiece, and the results were validated with copper electrodes. They identified that Ti electrodes have less degradation effect on the workpiece than copper electrodes did. Yadav et al. [3] used geometry-modified electrodes (e.g., slotted, helical, and tubular) in the EDM process. The influences of process parameters on the EDM performance were studied with the electrodes. They noted that the removal of machined products from the inter-electrode gap (IEG) for all tools had increased the machining rate and surface roughness

of work materials. Taherkhani et al. [4] investigated the EDM process parameters using Al_2O_3 particles mixed dielectrically in various concentration ranges on titanium alloy. The significant enhancement in machining surface was due to the prevention of oxides lever formation in the dielectric medium. Also, the presence of oxygen and carbon elements leads to uniform power distributions, which control crack formations over the machining surface. Phan et al. [5] experimented with an aluminium electrode in EDM process to determine its suitability on the titanium alloy. They optimized the process parameters using Taguchi method and obtained the maximum MRR 0.0239 g/min with less error. Ilani et al. [6] and [7] fabricated a tool in the technique of fused deposition modelling and employed EDM to improve the machining performance. The result was a tool using the surfactant stirred dielectrics such as with powder mixed and non-powder mixed electrolyte. They noted a 77 % improvement in surface roughness with this novel electrode. Also, this type of electrode is cost effective and makes the EDM functions easier for the production of complex geometries. Phan et al. [8] coated aluminium chromium nickel on an aluminium electrode to investigate the EDM parameters for titanium alloy. The experiments' results of a coated electrode are compared with a non-coated aluminium electrode. The coating of the aluminium in the electrode increases the material removal rate significantly; the coated electrode produces 24 % less TWR than the uncoated electrode does. Shaikh and Ahuja [9] conducted the experiments with electrodes, such as silver coated tungsten and electroless nickel coated electrodes, in the EDM process. They noted that the electroless nickel-coated electrode has a20 % higher machining rate than the silver-coated tool, which is because the electroless nickel coating increases the current distribution on the electrode. Walia et al. [10] studied the influences of a copper and titanium carbide mixed composite electrode on EDM with EN31 die steel. The copper composite electrode result reveals that the roundness of the hole was reduced around 25 % due to the electrode's conductance change. They mentioned that significant performance results in terms of MRR and surface roughness were obtained with the composite electrode than the plain copper electrode. Sahuand Mahaptra [11] prepared a aluminium, silicon, and magnesium mixed composite electrode through selective laser sintering method. They considered titanium as a workpiece and conducted the experiments using various tools, including composite, graphite, and copper electrodes. They obtained higher TWR and excellent surface roughness with the composite electrode than other tools. Mahipal Reddy et al. [12] employed a3D printing (i.e., direct metal laser sintering) to fabricate the aluminium composite electrode used in the EDM of steel alloy. The experiment results were compared with the commercial electrodes and performances were evaluated by means of MRR, TWR, and Servient et al. [13] used a rotary type tool in EDM of work material: high-speed steel through air mixed glycerine dielectric medium. The tool rotation speed, gas pressure, current, and dielectric flow rate were considered for the process parameters on the study of machining rate, overcut and surface roughness. They noted the improvement in the machining rate and surface roughness with the rotary tool electrode. Padhi et al. [14] used the additive manufacturing tool for machining the D2 steel using EDM. They coated the electrode with acrylonitrile-based polymer by fusion deposition method, which increased the electrical conductance of the electrode and increased the machining rate significantly. Mathai et al. [15] adopted the planetary tool movement on EDM to investigate the process parameters for titanium alloy. Along with this planter movement, they fabricated square holes with two types of electrodes materials (i.e., copper and graphite). Also, they noted that the copper tool produced better machining rate and surface finish than the graphite electrodes did. Wang et al. [16] tried two types of electrodes (i.e., cylindrical and helical) in a micro-EDM process on titanium alloy. The helical electrode increases the debris removal passage between tool and electrode, which increases the current flowability. This phenomenon ensures the high machining rate and better surface finish on the micro holes. Vincent and Kumar [17] used copper and brass rotary electrodes with EDM on En41b steel. They have noted less tool wear rate on the copper electrode than the brass electrode due to the current fluctuation on the IEG. Also, based on the analyses of variance, pulse on time and pulse off time played major role on the machining performance. Singh et al. [18] investigated the EDM performance using an air-associated rotary tool on high chromium die steel. They compared the experimental results with non-air assisted EDM under the same parameter setup. According to this, a high machining rate and less overcut was found on the air-assisted tool than the normal tool. Along with various techniques employed in EDM to enhance its performances (e.g., powder mixed dielectric [19], tool coating [20] and optimization of process parameters), using various techniques such as TOPSIS, Taguchi-data envelopment analysis-based ranking, Taguchi–grey relational analysis by the researchers [21] to [24].

The aforementioned literature clearly indicates that the various research methodologies have been followed by the researchers to enhance the EDM process. However, research on powder metallurgy-based tools on the EDM process is sparse. Although some researchers have considered PM tools in EDM, all the methods show poor surface finish and machining rate due to the improper reinforcements with Cu [25] to [27]. Titanium carbide and zirconium silicate particles possess an excellent affinity with Cu material due to their crystallographic nature. Hence, in this research, two electrodes in different reinforcement combinations (i.e., 90 % Cu, 5% TiC 5 % $ZrSiO_4$(Cu_{90}) and 80 % Cu, 5% TiC 5 % $ZrSiO_4$(Cu_{80})) are prepared using PM technique. The results of these tools are compared with plain Cu electrodes. With these three tools, EDM and its process parameters are optimized using TOPSIS and GRA methods. Furthermore, scanning electron microscope (SEM) image analyses are carried out for the better understanding of the effect of PM-based tools on machining performances.

1 EXPERIMENTAL SETUP

The experiments are conducted using a ZNC EDM machine, shown in Fig. 1. The tool electrode was prepared based on the powder metallurgy technique and hot extrusion method employed to diminish the porosity of the composite. The materials Cu- TiC-ZrSiO4 are used for the tool electrode preparation with various weight ratios, as shown in Table 1. The procedures for producing tool electrodes are followed from the literature [28] and explored in Fig. 2. The grain sizes of reinforcement particles are considered lower than 75 µm for all electrode samples. The composite electrodes of diameter 10 mm and 5 cm length are prepared. When considering various application of SS, in this attempt 5 mm thick SS 304 materials are used as work material.

Fig. 1. *EDM setup*

The machining parameters levels and experimental planning with outcomes are shown in Tables 2 and 3. L18 OA is planned with three tool electrodes: PC, PT, and GV. The SEM pictures of PM-based electrodes (i.e., Cu, Cu_{90}, and Cu_{80}) are shown in Figs. 3 to 5. The performances of EDM are estimated in terms of MRR, TWR, and SR. The commercially available dielectric medium kerosene is used for flushing between the tool and electrode. The machining times fixed as 30 minutes for all experiments, and levels of parameters are selected based on the literature [28]. Every completion of experimental workpieces and electrodes are cleaned using acetone to remove debris from the machining zone of workpiece. Before and after machining weights of tools and workpieces are

**Fig. 2.** *Powder metallurgy-based electrodes*

taken into the account for calculating the MRR and TWR, respectively [29]. The surface roughness of the machined area is measured using a surface roughness testing machine (Surf test SJ-210, Mitutoyo, Japan). Furthermore, SEM image analysis is carried out on the machined workpiece surfaces for a better understanding of the effect of tools on machining.

Table 1. *Weight ratios of electrode*

Electrodes type	Electrodes No	% of reinforcements		
		Cu	TiC	ZrSiO$_4$
Cu	Cu	100	-	-
Cu$_{90}$	Cu$_{90}$(TiC)$_5$(ZrSiO$_4$)$_5$	90	5	5
Cu$_{80}$	Cu$_{80}$(TiC)$_{10}$(ZrSiO$_4$)$_{10}$	80	10	10

Table 2. *Range of machining parameters*

Symbol	Machining parameters	Unit	L-1	L-2	L-3
A	Electrode type	-	Cu	Cu$_{90}$	Cu$_{80}$
B	Peak current	[A]	8	16	24
C	Pulse on	[µs]	15	30	45
D	Gap voltage	[V]	50	75	100
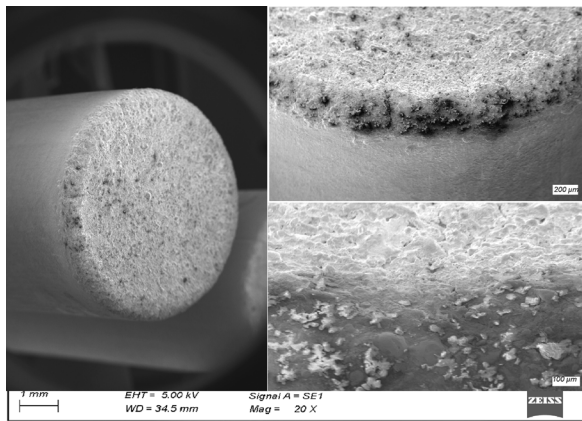
Fig. 3. *Plain Cu electrode (Cu)*
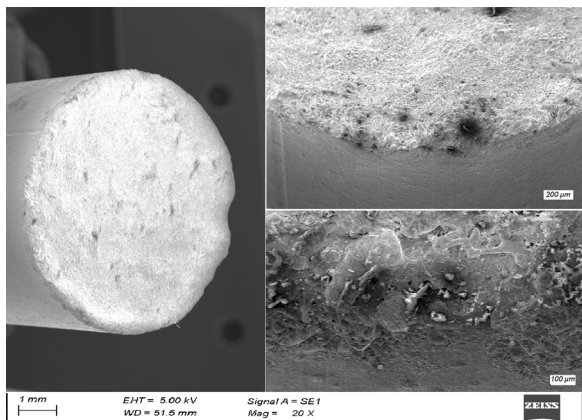
Fig. 4. Cu$_{90}$(TiC)$_5$(ZrSiO$_4$)$_5$ *electrode (Cu$_{90}$)*
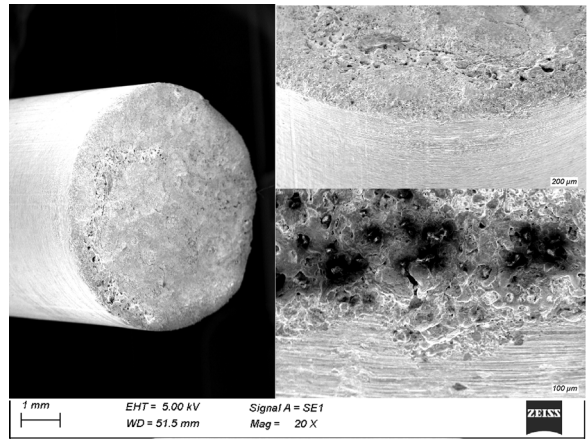
Fig. 5. Cu$_{80}$(TiC)$_{10}$(ZrSiO$_4$)$_{10}$ *electrode (Cu$_{80}$)*

Table 3. *Experimental planning*

Run	TE	PC	PT	GV	MRR [g/min]	TWR [g/min]	SR [µm]
1	1	8	15	50	0.0101	0.0533	4.12
2	1	16	30	75	0.0011	0.0253	4.39
3	1	24	45	100	0.0231	0.0538	5.27
4	2	8	15	75	0.0365	0.0451	5.89
5	2	16	30	100	0.0112	0.0423	6.92
6	2	24	45	50	0.0099	0.0266	5.87
7	3	8	30	50	0.0098	0.0451	5.94
8	3	16	45	75	0.0012	0.0296	6.12
9	3	24	15	100	0.0014	0.0091	7.14
10	1	8	45	100	0.0356	0.0478	7.82
11	1	16	15	50	0.0085	0.0225	7.18
12	1	24	30	75	0.0130	0.0489	8.23
13	2	8	30	100	0.0201	0.0589	7.87
14	2	16	45	50	0.0173	0.0149	8.12
15	2	24	15	75	0.0194	0.0412	8.94
16	3	8	45	75	0.0080	0.0072	8.15
17	3	16	15	100	0.0251	0.0188	7.25
18	3	24	30	50	0.0097	0.0419	8.92

1.1 Multi-objective Optimization

1.1.1 Technique for Order of Preference by Similarity to Ideal Solution (TOPSIS)

TOPSIS is an appropriate technique to identify the suitable parametric solution from the set-off experimental combinations. The procedures followed in this method are provided below [30] and [31].

Step 1: Choices of variables, i.e., all the responses are employed in the matrix in *n* attributes and *m* alternatives, which is shown with Eq. (1).

$$\mathbf{E_m} = \begin{bmatrix} R_{11} & R_{12} & R_{13} & \dots & R_{1n} \\ R_{21} & R_{22} & R_{23} & \dots & R_{2n} \\ R_{31} & R_{32} & R_{33} & \dots & R_{3n} \\ \vdots & \vdots & \vdots & \ddots & \vdots \\ R_{m1} & R_{m2} & R_{m3} & \dots & R_{mn} \end{bmatrix}, \tag{1}$$

where R_{ij} is the presentation of ith alternative with respect to jth attribute.

Step 2: Eq. (2) has been used for the normalization of matrix values, which can convert all values in a single form of units.

$$r_{ij} = \frac{R_{ij}}{\sqrt{\sum_{i=1}^{m} R_{ij}^2}}, \quad j = 1, 2, \dots, n. \tag{2}$$

Step 3: Weights for the output responses are assigned using Eq. (3) as $W_j(j = 1, 2, \dots, n)$. The preferences for outcome responses are assigned based on the requirement.

$$Y = W_j r_{ij}, \tag{3}$$

where, $\sum_{j=1}^{n} W_j = 1$.

Step 4: Suitable (best) ideal result is estimated using Eq. (4) and the worst ideal result is attained through Eq. (5).

$$Y^+ = \left\{ \left(\sum_i^{max} Y\,ij \mid j \in J \mid i = 1, 2, \dots, m \right) \right\}$$
$$= \left\{ y_1^+, y_2^+, y_3^+, \dots\dots, y_n^+ \right\}, \tag{4}$$

$$Y^- = \left\{ \left(\sum_i^{min} Y\,ij \mid j \in J \mid i = 1, 2, \dots, m \right) \right\}$$
$$= \left\{ y_1^-, y_2^-, y_3^-, \dots\dots, y_n^- \right\}. \tag{5}$$

Step 5: The value differences among the parameters are evaluated with the 'suitable ideal' solution is calculated using Eq. (6).

$$t_i^+ = \sqrt{\sum_{j=1}^{n} \left(Y_{ij} - y_j^+ \right)}, \quad i = 1, 2, \dots, m. \tag{6}$$

The deviation of experimental results from the 'worst–ideal' solution is calculated using Eq. (7).

$$t_i^- = \sqrt{\sum_{j=1}^{n} \left(Y_{ij} - y_j^- \right)}, \quad i = 1, 2, \dots, m. \tag{7}$$

Step 6: Eq. (8) used to find the closeness of various parameters solution which is presented below.

$$P_i = \frac{t_i^-}{t_i^+ + t_i^-}, \quad i = 1, 2, \dots, m. \tag{8}$$

Step 7: Obtained preference values (P_i) are ordered in a downward manner to identify the best parameter solution.

1.1.2 Grey Relational Analysis Technique (GRA)

With the GRA method, the output responses of different units should be converted into a homogeneous form (i.e., unit-less number). Therefore, the experimental results are converted from zero to one through the below-mentioned equations [30] and [31]. The output values (i.e., MRR, TWR and SR values) are estimated using Eqs. (9) and (10), respectively:

$$Y_i^*(P) = \frac{y_i(P) - \min y_i(P)}{\max y_i(P) - \min y_i(P)}, \tag{9}$$

where $i = 1, 2, \dots, m$, $P = 1, 2, \dots, n$,

$$y_i^*(P) = \frac{\max y_i(P) - y(P)}{\max y_i(P) - \min y_i(P)}, \tag{10}$$

where $i = 1, 2, \dots, m$, $P = 1, 2, \dots, n$.

Here, the equation contains m means the total number of experiments and n means received data. Eq. (11) is employed to estimate the grey relational coefficient (GRC) with the normalized values:

$$k_i(N) = \frac{\Delta_{min} + \zeta \Delta_{max}}{\Delta_{oi}(Q) + \zeta \Delta_{max}}. \tag{11}$$

Here, $\Delta_{oi}(Q)$ divergence series is chosen from the reference sequence $k(N)$ and comparability sequence $k_i^*(N)$. The range 0 to 1 has been used for the distinguished coefficient k_i.

$$T_i = \frac{1}{n} \sum_{P=1}^{n} j_i(N). \tag{12}$$

The weight values of each output response are in summation with GRC to find the grey relational grade (GRG) T_i is displayed in Eq. (12).

2 RESULT AND DISCUSSION

2.1 Influences of Input Parameters on MRR

The influences of the input parameters (i.e., electrode, peak current, pulse on time and gap voltage on MRR) are presented in Fig. 6. The experiments are conducted using three different tools, displayed in Table 3. The graphs are drawn according to the mean values of MRR against the input parameter values. It is clear from the figure that using composite tools exhibits higher MRR when compared to the plain copper tool, which produces 0.0319 g/min MRR. This value is 1.9 times higher than the existing composite tool used in the EDM process. The PM-based composite tools possess uneven surfaces at the end face tool with porosity. Hence, the passing of electric current has fast movement between the inter-electrode gap, which ensures higher MRR with the composite electrode [32]. Also, MRR is increased with the increasing percentage of titanium carbide and zirconium silicate in the composite tools. The softness of the composite tool is increased by the presence of zirconium silicate, which leads to high inter-metallic gaps among the particles. This phenomenon leads to better current conductance in the tool electrode and leads to the higher MRR.
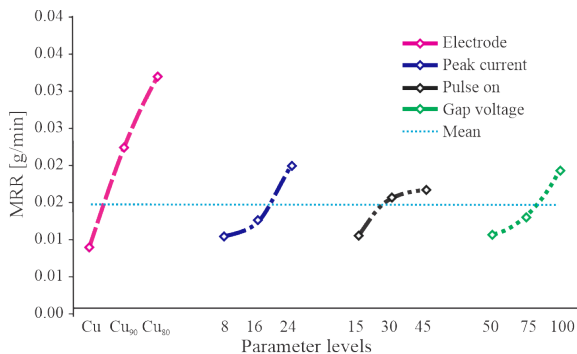

Fig. 6. *Influences of input parameters on MRR*

Moreover, from the figure, it is observed that increasing the peak current increases the MRR. It is a common fact that increasing the current with no flow disturbance in the electrode can produce the narrow power supply in the machining zone, which causes higher MRR [33]. The same trend of higher MRR has been obtained with the increasing of pulse on time and gap voltage. The timing of current passage and flow ability increases at higher level, which leads to the higher MRR for all tools.

2.2 Influences of Input Parameters on TWR

The effect of input parameters on TWR is displayed in Fig. 7. The figure shows that PM-based tools produce lower TWR (0.0234 g/min) when there is an increase in the percentage of titanium carbide and zirconium silicate. Increasing the percentage of compositions increases the wear resistance among particles and increases the porosity of the tools. Therefore, the connectivity of the current is disbursed when it is applied to the machining zone [34]. This character of tool electrodes leads to less TWR on PM tools at higher levels of parameter combinations. However, the percentage of titanium carbide and zirconium silicate at the middle stage electrode (i.e., 5 % TiC and 5 % $ZrSiO_4$) shows the increased TWR with increasing of parametric range. It is because titanium carbide provides the additional energy to the electrode to pass the current by its conductivity nature. Therefore, the middle stage of composite electrodes produces the higher TWR. , due to the high spark energy of tool, higher TWR has been obtained with the higher peak current, pulse on time and gap voltages.
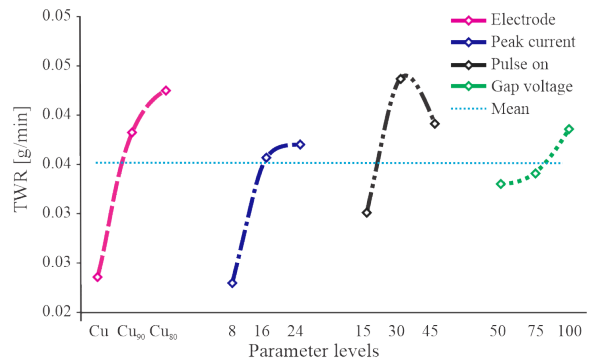

Fig. 7. *Influences of input parameters on TWR*

2.3 Influences of Input Parameters on SR

The effect of input parameters on the SR is displayed in Fig. 8. The SR shows the increasing trend with increases in parameters values. Better surface finish is observed with plain copper tool, producing the surface finish in the range of 6.16 μm to 7.04 μm, which is lower than other PM-based composite tools.

The PM composite tool produces crater surfaces, and it becomes the cause of higher MRR. The higher craters exhibit less surface finish and elements of the tool transferred over the machined surfaces. Hence, the surface finish of the machined area leads to the poor quality with PM composite tools than plain copper tool [35]. Also, the increasing of peak current, pulse on time, and gap voltage cause increasing spark

energy on the machining zone, which leads the excess material removal on the work material [36]. The SEM image of the machined area are shown in Figs. 9 and 10 for first and second optimal combinations. Furthermore, the machined products (debris) are deposited over the crater surface due to the improper flushing and form the recast layer on the machined surface.
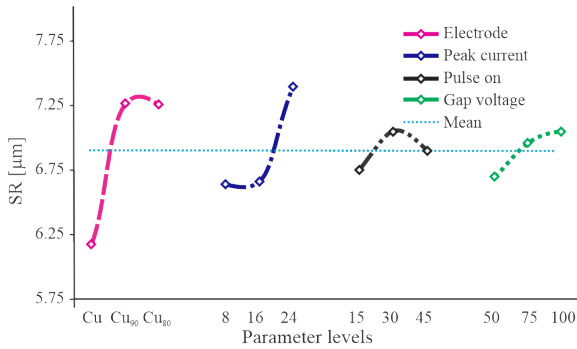

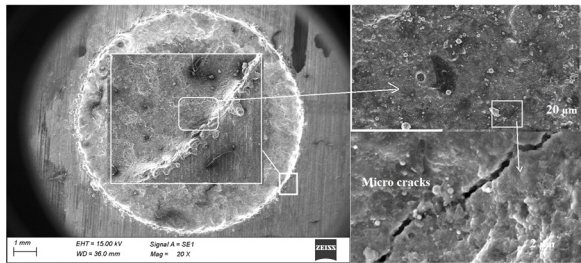**Fig. 8.** *Influences of input parameters on SR*

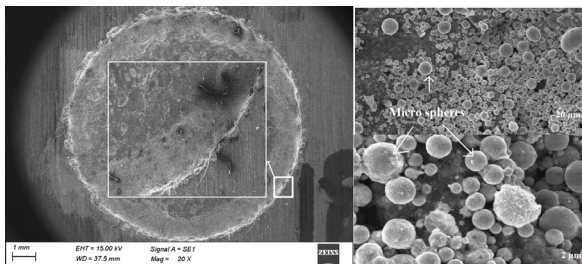**Fig. 9.** *SEM image of 1st optimal combination*

Fig. 10. *SEM image of 2nd optimal combination*

2.4 TOPSIS

The output values of EDM such as MRR, TWR and SR through PM based tools are optimized using the TOPSIS technique. Eqs. (1) to (8) have been used to obtain the preference value for the experimentations. Equal weights are assigned to all output responses under ideal conditions. The preferences values (Pi) and their ranking orders are represented in Table 4. The outcomes of the research are converted from

multi-objective optimization to single attribute optimization through combined methods of Taguchi and TOPSIS. The furthest preference value is termed as optimal parameter solution and the maximum rank is considered as the first optimal solution. Therefore, it is observed that the 17th experimental run (0.6735) is chosen as the best optimal parameter solution for the best performance of EDM due to the highest Pi value. The experimental runs 4th (0.6714) and 10th (0.6259) show the second and third best optimal parameter combinations. Hence, the best optimal solution is found to be the $Cu_{90}(TiC)_5(ZrSiO_4)_5$ PM-based tool, E8 Amp peak current, 15 μs pulse on time and 75 V gap voltage using TOPSIS.

Table 4. *TOPSIS ranking*

Experiment No.	Yi +	Yi –	Pi (Preference value)	Rank
1	0.4504	0.2039	0.3116	13
2	0.4836	0.2561	0.3462	12
3	0.3388	0.3187	0.4847	5
4	0.2393	0.4890	0.6714	2
5	0.4100	0.1815	0.3068	14
6	0.3777	0.2520	0.4002	8
7	0.4281	0.1752	0.2904	16
8	0.4933	0.2032	0.2917	15
9	0.4773	0.3111	0.3946	9
10	0.2779	0.4649	0.6259	3
11	0.3970	0.2512	0.3876	10
12	0.4263	0.1713	0.2866	17
13	0.4042	0.2556	0.3874	11
14	0.2920	0.3462	0.5425	4
15	0.3479	0.2664	0.4337	7
16	0.4014	0.3309	0.4519	6
17	0.1972	0.4068	0.6735	1
18	0.4450	0.1545	0.2578	18

2.6 Table of ANOVA for TOPSIS

ANOVA is a prominent method to determine the important and insignificant factors. The Pi values of PM-based tools are statically analysed using ANOVA, and the influences of each parameter over the output responses are examined. In addition, the F-test outcomes are used to identify the most important factor to attain better performance. Table 5 shows that pulse on time plays a major role, which contributes around 46.8 % to the machining performance. The next important factor is the tool electrode, which controls the machining performances, contributing about 27.7 %.

Table 5. *Table of ANOVA for TOPSIS*

Machining parameter symbol	DOF	SS	MS	F-test	% Contri
TE	2	0.0835	0.0418	2.9863	27.76
PC	2	0.0417	0.0209	1.4913	13.86
PT	2	0.1410	0.0705	5.0434	46.89
GV	2	0.0123	0.0062	0.4406	4.09
E	9	0.1258	0.0140		7.38
Total	17	0.4044	0.0238		100

2.7 GRA

In GRA method, outcomes of EDM (i.e., MRR, TWR, and SR) for various tools are normalized using Eqs. 9 and 10. Eqs. 11 and 12 are used to determine the GRC and GRG, respectively, for all conducted experiments. Equal weights are assigned for all responses. GRG and its rankings are displayed in Table 6. The furthest GRG value has been considered the optimal parameter solution. Therefore, based on the table, the 4th experimental run (0.7887) is the best optimal parameter solution, and the 17th (0.7868) and 16th (0.7773) experimental runs are the next best optimal parameter solutions through GRA method. Hence, the optimal parameter solution found to be $Cu_{90}(TiC)_5$ $(ZrSiO_4)_5$ PM-based tool, 8 A peak current, 15 μs pulse on time and 75 V gap voltage using GRA.

2.7 Table of ANOVA for GRG

The GRG results of various tools are statically analysed using ANOVA, presented in Table 7. The outcomes of results for PM based tools are optimized using the GRA method.

Therefore, peak current shows the most significant contribution around 39.3 % on machining performance.

The next significant parameter is pulse on time, which contributes on performances around 36.8 %.

The ranking values of TOPSIS and GRA technique are presented as a graph in Figure 8, which is plotted for experimental run vs. TOPSIS and GRA values. The 4th and 17th experimental runs show the first two optimal combinations for the best performance of EDM using the TOPSIS and GRA methods. Moreover, in both techniques, they provide the same parametric combination for machining. Also, the 10th and 16th experimental runs show the third optimal combinations using the TOPSIS and GRA methods.

Table 6. *GRG ranking*

Experiment No.	GRC			GRG	Rank
	MRR	TWR	SR		
1	0.5729	0.5286	1.0000	0.5508	18
2	0.5000	0.7407	0.9470	0.6204	11
3	0.7254	0.5258	0.8074	0.6256	10
4	1.0000	0.5773	0.7314	0.7887	1
5	0.5832	0.5955	0.6325	0.5894	14
6	0.5708	0.7279	0.7336	0.6493	8
7	0.5703	0.5771	0.7259	0.5737	17
8	0.5007	0.6984	0.7067	0.5996	12
9	0.5023	0.9651	0.6148	0.7337	6
10	0.9745	0.5603	0.5657	0.7674	4
11	0.5585	0.7725	0.6117	0.6655	7
12	0.6010	0.5536	0.5398	0.5773	16
13	0.6839	0.5000	0.5624	0.5919	13
14	0.6484	0.8708	0.5465	0.7596	5
15	0.6742	0.6037	0.5000	0.6389	9
16	0.5545	1.0000	0.5446	0.7773	3
17	0.7568	0.8167	0.6063	0.7868	2
18	0.5691	0.5983	0.5010	0.5837	15

Table 7. *Table of ANOVA for GRG*

Machining parameter symbol	DOF	SS	MS	F test	% Contri
TE	2	0.0098	0.0049	0.284	8.03
PC	2	0.0479	0.024	17.20	39.30
PT	2	0.0449	0.0225	16.12	36.82
GV	2	0.0068	0.0034	2.43	5.56
E	9	0.0125	0.0014		10.27
Total	17	0.1219	0.0072		100
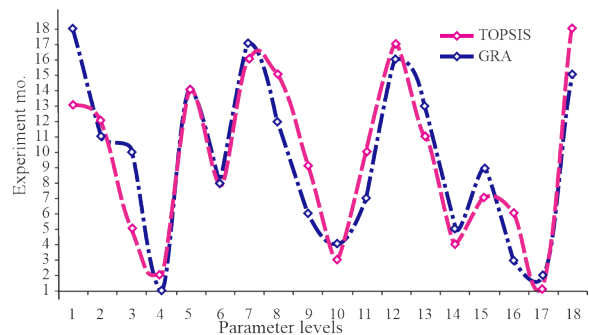
Fig. 11. *Comparison of TOPSIS and GRA ranking*

3 CONCLUSIONS

This research work aims to explore the benefits and performance measures of powder metallurgy-based copper electrodes in the EDM process. Two electrodes in different reinforcement combinations (i.e.,

$Cu_{90}(TiC)_5(ZrSiO_4)_5$ and $Cu_{80}(TiC)_{10}(ZrSiO_4)_{10}$ are prepared using a PM technique, and their results are compared with a plain Cu electrode. The experiments are conducted based on the L-18 OA, and optimization techniques (e.g., TOPSIS and GRA) are used to find the optimal solution.

The results show that MRR and TWR increase with increasing of the percentage of reinforcements in the composite electrodes. The Cu_{90} (Copper composite) tool electrode exhibits 0.0319 g/min MRR and this value is 1.9 times higher when compared to the existing tool electrode. The TOPSIS and GRA optimization techniques produce the same optimal parametric solution for lesser TWR, SR and higher MRR. Hence, the 17th experimental run is proposed as optimal parameter combination: $Cu_{90}(TiC)_5(ZrSiO_4)_5$, E8 Amp peak current, 15 µs pulse on time and 75 V gap voltage. In addition, based on the ANOVA table of TOPSIS, pulse on time plays a major role, contributing around 46.8 % tp the machining performance, and peak current shows the most significant contribution of around 39.3 % on machining performance using GRA values.

Therefore, the Cu_{90} composite tool is more appropriate for the higher MRR and less TWR. Furthermore, experiments can be conducted with various concentrations of reinforcements and different work materials to understand the behaviour of machining.

4 REFERENCES

[1] Sivakumar, K., Kumar, P.M., Amarkarthik, A., Jegadheeswaran, S., Shanmugaprakash, R. (2021). Empirical modeling of material removal rate and surface roughness of OHNS steel using Cu-TiB2Tool in EDM. *Materials Today: Proceedings*, vol. 45, part 2, p. 2725-2729, **DOI:10.1016/j.matpr.2020.11.597**.

[2] Chakmakchi, M., Ntasi, A., Mueller, W. D., Zinelis, S. (2021). Effect of Cu and Ti electrodes on surface and electrochemical properties of Electro Discharge Machined (EDMed) structures made of Co-Cr and Ti dental alloys. *Dental Materials*, vol. 37, no. 4, p. 588-296, **DOI:10.1016/j.dental.2021.01.012**.

[3] Yadav, V.K., Singh, R., Kumar, P., Dvivedi, A. (2021) Performance enhancement of rotary tool near-dry EDM process through tool modification. *Journal of Brazilian Society of Mechanical Sciences and Engineering*, vol. 43, art. ID 72, **DOI:10.1007/s40430-021-02806-y**.

[4] Taherkhani, A., Ilani, M.A., Ebrahimi, F., Huu, P.N, Long, B.T., Dong, P.V., Tam, N.C., Minh, N.D., Duc, N.V. (2021).Investigation of surface quality in cost of goods manufactured (COGM) method of µ-Al2O3 powder-mixed-EDM process on machining of Ti-6Al-4V. *International Journal of Advanced Manufacturing Technology, vol.* 116, p. 1783-1799, **DOI:10.1007/s00170-021-07573-7**.

[5] Phan, N.H., Pi, V.N., Shirguppikar, S., Patil, M.S., Ilani, M.A., Hung, L.X., Hung, T.Q. (2020). Material removal rate in electric discharge machining with aluminum tool electrode for Ti-6Al-4V titanium alloy. *International Conference on Engineering Research and Applications*, p. 527-533, **DOI:10.1007/978-3-030-64719-3_58**.

[6] Ilani, M.A., Khoshnevisan, M. (2021). Study of surfactant effects on intermolecular forces (IMF) in powder-mixed electrical discharge machining (EDM) of Ti-6Al-4V. *The International Journal of Advanced Manufacturing Technology*, vol. 116, p. 1763-1782, **DOI:10.1007/s00170-021-07569-3**.

[7] Ilani, M.A., Khoshnevisan, M. (2020). Powder mixed-electrical discharge machining (EDM) with the electrode is made by fused deposition modeling (FDM) at Ti-6Al-4V machining procedure. *Multiscale and Multidisciplinary Modeling, Experiments and Design*, vol. 3, p. 173-186, **DOI:10.1007/s41939-020-00070-6**.

[8] Phan N.H., Pi, V.N., Tuan, N.G., Shirguppikar, S., Patil, M.S., Ilani, M.A., Hung, L.X., Muthuramalingam, T., Hung, T.Q. (2021) Tool wear rate analysis of uncoated and AlCrNi coated aluminum electrode in EDM for Ti-6Al-4 V titanium alloy. *Advances in Engineering Research and Application. Lecture Notes in Networks and Systems*, vol. 178, **DOI:10.1007/978-3-030-64719-3_91**.

[9] Shaikh, M.S.N.M., Ahuja, B.B. (2020). Effects of primary and secondary metallization techniques on the performance of electric discharge machining (EDM) electrode produced by additive manufacturing and composite coating. *Materials Today: Proceedings*, vol. 41, part, 4, p. 874-885, **DOI:10.1016/j.matpr.2020.09.441**.

[10] Walia, A.S., Srivastava, V., Jain, V., Bansal, S.A. (2020). Effect of Tic reinforcement in the copper tool on roundness during EDM process. *Advances in Materials Science and Engineering, Lecture Notes in Mechanical Engineering*, p. 125-135, **DOI:10.1007/978-981-15-4059-2_10**.

[11] Sahu, A.K., Mahapatra, S.S. (2020). Performance analysis of tool electrode prepared through laser sintering process during electrical discharge machining of titanium. *The International Journal of Advanced Manufacturing Technology*, vol. 106, p. 1017-1041, **DOI:10.1007/s00170-019-04675-1**.

[12] Mahipal Reddy, L., Siva Rama Krishna, L., Sharath Kumar, S., Ravinder Reddy, P. (2020). A comparative study on performance of 3D-Printed EDM electrode with conventional EDM electrode. *Recent Trends in Mechanical Engineering. Lecture Notes in Mechanical Engineering*, p. 217-225, **DOI:10.1007/978-981-15-1124-0_19**.

[13] Yadav, V.K., Kumar, P., Dvivedi, A. (2019). Effect of tool rotation in near-dry EDM process on machining characteristics of HSS. *Materials and Manufacturing Processes*, vol. 34, no. 7, p. 779-790, **DOI:10.1080/10426914.2019.1605171**.

[14] Padhi, S.K., Mahapatra, S.S., Padhi, R., Das, H.C. (2018). Performance analysis of a thick copper-electroplated FDM ABS plastic rapid tool EDM electrode. *Advances in Manufacturing*, vol. 6, p. 442-456, **DOI:10.1007/s40436-018-0238-5**.

[15] Mathai, V.J., Dave, H.K., Desai, K.P. (2017). Experimental investigations on EDM of Ti6Al4V with planetary tool actuation. *Journal of Brazilian Society of Mechanical Sciences and*

Engineering, vol. 39, p. 3467-3490, **DOI:10.1007/s40430-016-0657-9**.

[16] Wang, K., Zhang, Q., Zhu, G., Liu, Q., Huang, Y. (2017). Experimental study on micro electrical discharge machining with helical electrode. *International Journal of Advanced Manufacturing and Technology*, vol. 93, p. 2639-2645 **DOI:10.1007/s00170-017-0747-6**.

[17] Vincent, N., Kumar, A.B. (2016). Experimental investigations into EDM behaviours of En41b using copper and brass rotary tubular electrode. *Procedia Technology*, vol. 25, p. 877-884. **DOI:10.1016/j.protcy.2016.08.196**.

[18] Singh, N.K., Pandey, P.M., Singh, K.K. (2015). EDM with an air-assisted multi-hole rotating tool. *Materials and Manufacturing Processes*, vol. 31, no. 14, p. 1872-1878, **DOI:10.1080/10426914.2015.1127954**.

[19] Banh, T.L., Nguyen, H.P., Ngo, C., Nguyen, D.T. (2018). Characteristics optimization of powder mixed electric discharge machining using titanium powder for die steel materials. *Proceedings of the Institution of Mechanical Engineers, Part E: Journal of Process Mechanical Engineering*, vol. 232, no. 3, p. 281-298, **DOI:10.1177/0954408917693661**.

[20] Phan, N.H., Dong, P.V., Muthuramalingam, T., Thien, N.V., Dung, H.T., Hung, T.Q., Ly, N.T. (2021). Experimental investigation of uncoated electrode and PVD AlCrNi coating on surface roughness in electrical discharge machining of Ti-6Al-4V. *International Journal of Engineering*, vol. 34, no. 4, p. 928-934, **DOI:10.5829/IJE.2021.34.04A.19**.

[21] Nguyen, H.P., Pham, V.D., Ngo, N.V. (2018). Application of TOPSIS to Taguchi method for multi-characteristic optimization of electrical discharge machining with titanium powder mixed into dielectric fluid. *The International Journal of Advanced Manufacturing Technology*, vol. 98, no. 5, p. 1179-1198, **DOI:10.1007/s00170-018-2321-2**.

[22] Sundriyal, S., Vipin, V.,Walia, R.S. (2020). Study on the influence of metallic powder in near-dry electric discharge machining. *Strojniški vestnik - Journal of Mechanical Engineering*, vol. 66, no. 4, p. 243-253, **DOI:10.5545/sv-jme.2019.6475**.

[23] Sundriyal, S., Vipin, V., Walia, R. S. (2020). Experimental Investigation of the micro-hardness of EN-31 die steel in a powder-mixed near-dry electric discharge machining method. *Strojniški vestnik- Journal of Mechanical Engineering*, vol. 66, no. 3, p. 184-192, **DOI:10.5545/sv-jme.2019.6474**.

[24] Yuvaraj, T., Suresh, P. (2019). Analysis of EDM process parameters on inconel718 using the Grey-Taguchi and Topsis methods. *Strojniški vestnik - Journal of Mechanical Engineering*, vol. 65, no. 10, p. 557-565, **DOI:10.5545/sv-jme.2019.6194**.

[25] Sahu, A.K., Mahapatra, S.S. (2020). Performance analysis of Cu-W-B4C composite tool during electrical discharge machining of titanium alloy. *Proceedings of the Institution of Mechanical Engineers, Part C: Journal of Mechanical Engineering Science*, vol. 235, no. 11, p. 1992-2007, **DOI:10.1177/0954406220951597**.

[26] Patowari, P.K., Saha, P., Mishra, P.K. (2011). Taguchi analysis of surface modification technique using W-Cu powder metallurgy sintered tools in EDM and characterization of the deposited layer. *The International Journal of Advanced Manufacturing Technology*, vol. 54, p. 593-604, **DOI:10.1007/s00170-010-2966-y**.

[27] Tsai, H.C., Yan, B.H., Huang, F. Y. (2003). EDM performance of Cr/Cu-based composite electrodes. *International Journal of Machine Tools and Manufacture*, vol. 43, no.3, p. 245-252, **DOI:10.1016/S0890-6955(02)00238-9**.

[28] Sahu, A.K., Mahapatra, S.S. (2020). Prediction and optimization of performance measures in electrical discharge machining using rapid prototyping tool electrodes. *Journal of Intelligent Manufacturing*, p. 1-21, **DOI:10.1007/s10845-020-01624-8**.

[29] Ilani, M.A., Khoshnevisan, M. (2021). Mathematical and physical modeling of FE-SEM surface quality surrounded by the plasma channel within Al powder-mixed electrical discharge machining of Ti-6Al-4V. *The International Journal of Advanced Manufacturing Technology*, vol. 112, p. 3263-3277, **DOI:10.1007/s00170-021-06626-1**.

[30] Soundarrajan, M., Thanigaivelan, R. (2018). Investigation on electrochemical micromachining (ECMM) of copper inorganic material using UV heated electrolyte. *Russian Journal of Applied Chemistry*, vol. 91, p. 1805-1813, **DOI:10.1134/S1070427218110101**.

[31] Soundarrajan, M., Thanigaivelan, R. (2019). Investigation of electrochemical micromachining process using ultrasonic heated electrolyte. *Advances in Micro and Nano Manufacturing and Surface Engineering, Lecture Notes on Multidisciplinary Industrial Engineering*, p. 423-434, **DOI:10.1007/978-981-32-9425-7_38**.

[32] Khanra, A.K., Sarkar, B.R., Bhattacharya, B., Pathak, L.C., Godkhindi, M.M. (2007). Performance of ZrB$_2$-Cu composite as an EDM electrode. *Journal of Materials Processing Technology*, vol. 183, no. 1, p. 122-126, **DOI:10.1016/j.jmatprotec.2006.09.034**.

[33] Soundarrajan, M., Thanigaivelan, R. (2020). Effect of coated and geometrically modified tools on performance of electrochemical micromachining. *Materials and Manufacturing Processes*, vol. 35, no. 7, p. 775-782, **DOI:10.1080/10426914.2020.1740252**.

[34] El-Taweel, T.A. (2009). Multi-response optimization of EDM with Al-Cu-Si-TiC P/M composite electrode. *The International Journal of Advanced Manufacturing Technology*, vol. 44, p. 100-113, **DOI:10.1007/s00170-008-1825-6**.

[35] M.S. Shunmugam, P.K. Philip, Gangadhar, A. (1994). Improvement of wear resistance by EDM with tungsten carbide P/M electrode. *Wear*, vol. 171, no. 1-2, p. 1-5, **DOI:10.1016/0043-1648(94)90340-9**.

[36] Singh, S., Maheshwari, S., Pandey, P.C. (2004). Some investigations into the electric discharge machining of hardened tool steel using different electrode materials, *Journal of Materials Processing Technology*, vol. 149, no. 1-3, p. 272-277, **DOI:10.1016/j.jmatprotec.2003.11.046**.